Computers and Electronics in Agriculture
25 (2000) 29–51

Computers and electronics in agriculture

www.elsevier.com/locate/compag

A guidance-assistance system for agricultural vehicles

C. Debain [a,*], T. Chateau [a], M. Berducat [a], P. Martinet [b], P. Bonton [b]

[a] *CEMAGREF* [1], *24 Avenue des Landais, 63172 Aubiere Cedex, France*
[b] *LASMEA* [2], *24 Avenue des Landais, 63177 Aubiere Cedex, France*

Abstract

This article presents a guidance-assistance system for agricultural machines. It is based on analysis of the vehicle's environment by image processing to deduce a control law in the image space. Two algorithms of image processing and two control laws are presented. It presents some results of crop edge detection and control of the vehicle's trajectory in several conditions. These results show the feasibility of such a project and the necessity to know the reliability of the image processing results to secure the viability of the complete system.

Keywords: Guidance system; Image processing; Visual servoing; Texture analysis; Control; Agricultural vehicles

1. General introduction

Working on new equipment to increase agricultural productivity and safety, reducing the difficulties of human tasks, CEMAGREF and LASMEA have developed a guidance-assistance system for agricultural vehicles. The aim of this system is to help the operator to guide the machine in order to give more attention to the control of other functions. To reach this aim, we use a visual perception of the environment because this method of sensing gives a solution well-adapted to many

* Corresponding author. Tel.: +33-473-440681.
E-mail address: christophe.debain@cemagref.fr (C. Debain)
[1] Agricultural and Environmental Engineering Research.
[2] Automatic and Electronic Laboratory in Blaise Pascal University.

PII: S0168-1699(99)00054-X

situations. This project began with research on a visual guidance-assistance system for a mower in 1991 and has been adapted to the development of the same system for a combine harvester in 1995. Several works on guidance-assistance systems in agriculture in the world have been published during the 1990s (Jarvis, 1990; Nobutaka, 1990; Amat et al., 1993; Klassen et al., 1994; Ollis and Stentz, 1996, 1997; Billingsley and Schoenfisch, 1997; Marchant et al., 1997; Sanchez and Marchant, 1997). We particularly notice the work of M. Ollis on the Demeter project at Carnegie Mellon University (Ollis and Stentz, 1996, 1997). The most important problem in these applications is to extract information about vehicle environment in difficult conditions found in agriculture (vegetation, sunshine conditions, relief). So in the first part of this paper, we present two environment perception methods used to guide a mower or a combine harvester. In the second part we detail two control laws applied to agricultural vehicles.

2. Image processing

2.1. Introduction

Within the framework of the guidance-assistance of an agricultural vehicle, and especially along a crop edge, CEMAGREF and LASMEA have amassed important experience for many years. Thus, the brief comments which follow concerning the problematic characteristics of a vision system in the agricultural environment, specially in relation to plant cover, partly explain the research orientation of the team at Clermont-ferrand (Derras et al., 1994). The first stage of this work consisted of experiments needed to characterize the environment. The acquisition of an important bank of images has made it possible to measure the effect of different parameters such as the variation of the sunshine conditions, the density and the type of crop cover. The first observation from these studies was the significant variability of image luminance. So we have chosen both parameters of luminance and texture as the best criteria for characterizing images. The second observation was the undesirable effect of the shadow generated by the vegetation, particularly the appearance of a dark area between the cropped zone and the uncropped zone.

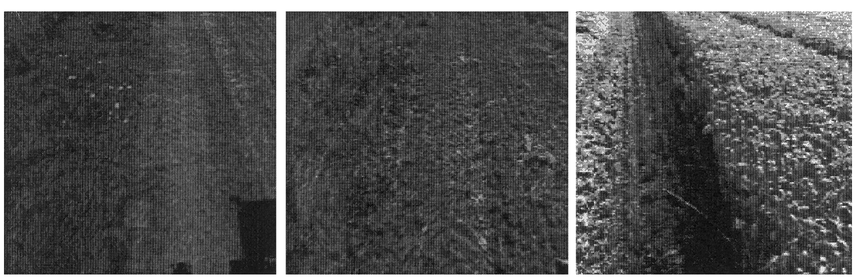

Fig. 1. Problem of outdoor vision: three images with different positions of the sun.

Fig. 1 illustrates the previous point. In the left picture, the acquisition was done in a configuration where the sun was positioned behind the sensor. In this case, the luminance is a good parameter in order to extract the position of the crop edge. In the middle picture, in which the only modification was the position of the sun (in front of the sensor), there is a notable absence of contrast. In this case, we have to use texture parameters so as to find the crop edge. The right picture is an example of a shadow caused by the vegetation. To segment these images, we use two different methods: the first is an unsupervised segmentation by Markov fields and the second is a supervised method which employs a reliability criterion in the segmentation.

2.2. Example of unsupervised method

To be independent of the region number in the image and the many situations found in a natural environment, we have developed an unsupervised segmentation algorithm using Markov fields (Derras et al., 1994).

2.2.1. Parameters

As we have explained in the introduction of this section, two types of parameters made up the input data of the Markov fields:

- two grey level parameters which are the maximum of the histogram and the second moment,
- two texture parameters which are the entropy and the homogeneity.

In order to chose these four descriptors, we have tested many image parameters. We mainly used the Haralick method (Haralick, 1979) based on co-occurrence matrices, in which the principal aim is to provide a good representation of the concept of grey level interactions. The constraints of a final application in a real time system has been integrated (sampling period: 100 ms) into the choice of the parameters. This explains why we have only considered parameters which need a low algorithm complexity. Let us consider I, an image with a size of $I_x^* I_y$ pixels. It can be divided into $n*m$ sites with a size of $S_x = I_x/\mathrm{m}$ and $S_y = I_y/n$. Let P_1, P_2, P_3, P_4, be four matrices with a size of $n*m$, which represent the maximum of the histogram, the second moment, the homogeneity and the entropy, computed for each site. Fig. 2, (where $I_x = 512$, $I_y = 128$, $m = 32$ and $n = 8$; so $S_x = S_y = 16$) illustrates this point. Fig. 2(a) is an example of an mowed/unmowed image. Fig. 2(b–e) are grey levels representation of the four parameters. In this example, we can see that only two parameters seem to be good for the estimation of the crop edge (the maximum of the histogram and the entropy). But, statistically, all the parameters are useful to segment the natural images met in our applications.

2.2.2. Markov segmentation, analysis and choice of the crop edge

Concerning the segmentation step, the use of Markov fields, and especially of the ICM (Iterated Conditional Mode) algorithm (Cohen and Cooper, 1987) gives good results. For instance in Fig. 3, we can see five regions which make it possible to find the crop edge. A list of all possible limits is extracted by a contour analysis module.

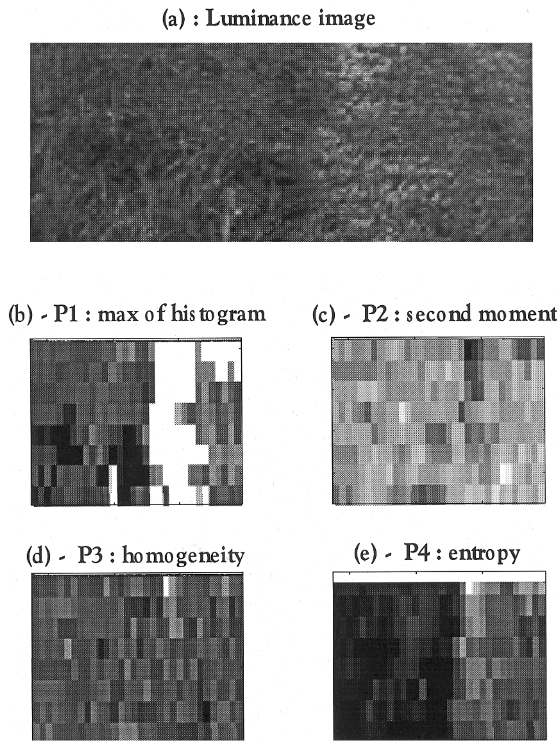

Fig. 2. Image parameters.

Fig. 3. Segmentation result.

The last part consists of the choice of the good limit in the list and its modeling by a straight line whose polar coordinates are (ρ and θ). It is made by minimization of an Euclidean distance criterion between all possible paths of the list and the result of the previous image. This last part of the algorithm is empirically right but wrong detections can appear resulting from shadow or from the tire tracks of the previous row. The theory and the implementation on a Real Time architecture are developed in (Derras et al., 1991; Derras, 1993).

2.2.3. Implementation and tests

Implemented in a real time system based on two 68060 microprocessors, the crop edge algorithm detection has an average time of execution which is about 100 ms per image (in 1997). Nevertheless the segmentation by Markov fields, which is not determinist, leads to the need for time limited security in order to avoid possible oscillations. This aspect appears as an important disadvantage in a real time based mode. One of the conclusions of our tests of this approach concerns the importance of the reliability of each crop edge estimation. In spite of a high percentage of good estimations (90%), determined by a human operator, the guidance is not reliable enough. As a matter of fact, we have to be able to quantify the uncertainty for each estimation in order to isolate the bad detection of the perception module.

2.3. Supervised algorithm

On the assumption that the scene contains only two classes (a cut and an uncut one), we can define a typical model of the image. The methods which use this model seem to be weakest, in contrast to the type of specific pictures than the algorithm based on the Markov fields segmentation. On the other hand, it is possible to quantify the similarity of the scene with this model in order to estimate the reliability of the detected limit. This point is essential and more important than the global performances of the algorithm so as to provide a good guidance in an iterative structured environment (the current environment is structured by the previous trajectory of the machine). The supervised method presented in this part provides both the position of the crop edge and the reliability criterion associated. It can be divided into three parts:

- a correlation function between the model and the real image is perform for each parameter,
- each correlation function is analyzed in order to quantify the reliability,
- the theory of evidence (Shafer, 1976) makes it possible to merge the information collected after the transformation of the correlation function into a mass function. The position of the crop edge is calculated through a maximum of belief rule. An estimation of a reliability criterion, associated with the detected position of the crop edge is performed and can be used in order to validate the result (Chateau et al., 1997).

2.3.1. The correlation approach

We assume that the straight line model of the crop edge is a nearly vertical line in the image plane. So, we sum by row each matrix $P_j\, j \in [1, 4] \subset N$ and we obtain a vector L_j, $j \in [1, 4] \subset N$ (each L_j has a dimension of m, and m is the P_j column number; like it is calculated in Section 2.2.1) in which the crop edge, materialized by a step transition, appears with less noise than in the 2D matrix. This transformation is realized by the following equation:

$$L_j = \frac{1}{n}(M.P_j) \tag{1}$$

where $M = \overbrace{(1, \ldots, 1)}^{n}$ representing a vector of n elements (n is the number of sites). Fig. 4 is a representation of L_1 in the example of the Fig. 2. The estimation of the position of the step can be performed by computing the deviation for each vector L_j; but this method is not adapted to noisy signals. W.Y. Liu proposed an operator for the detection of transitions in a very noisy signal. It is based on the local properties of stationarity of the signal (Liu, 1994). The approach described here is based on performing a correlation function computing between vector L_j and a reference vector G (a step transition). The correlation function between the two vectors is defined by (Max, 1985):

$$\mathrm{Corr}_{L_j G}(x) = \frac{1}{m+1} \sum_{k=0}^{m} L_j(k).G(k-x) \tag{2}$$

Let us define the reference vector G by:

$$G = \left(\underbrace{-\alpha, \ldots -\alpha}_{\beta.m} \; \underbrace{\alpha, \ldots .\alpha}_{\beta.m} \; \underbrace{0, \ldots 0}_{1-2.\beta.m} \right) \tag{3}$$

with $\beta \in [0, 0.5] \subset R$ and $\alpha = 1$ or -1.

We define α as the crop edge characteristic coefficient. It is an a priori component of the algorithm. In our application, $\alpha = 1$ and $\beta = 5/m$.

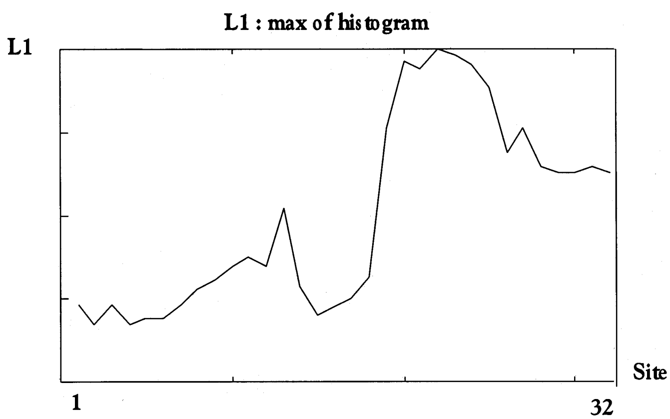

Fig. 4. Matrix L_1.

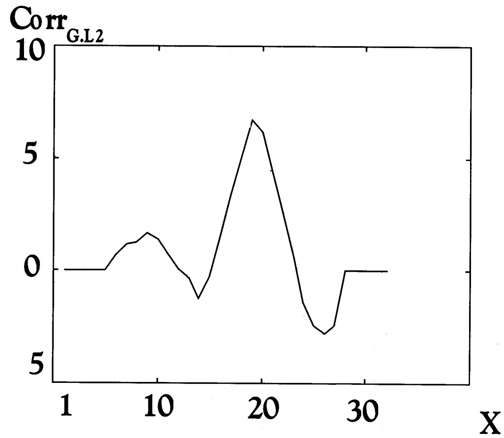

Fig. 5. Correlation function.

We have to remove the mean value of L_j before computing the correlation function between the measured signal and the sought pattern. The position of the maximum of the function Corr_{L_jG} is the most probable position of the search pattern in the initial signal. We can deduce the position of the crop edge from this information. Fig. 5 is a representation of the correlation function computing from L_2.

2.3.2. *Data fusion*

The previous part describes a method which performs some correlation functions associated with the luminance and texture parameters. Now, all these functions must be merged in order to estimate a more probable position of the crop edge.

2.3.2.1. Estimation of the uncertainty. If I is a perfect image with two parts and no noise, the correlation function presents only one maximum which the value is $\mu_a/m = 2.\beta$ with $\mu_a = \max(\mathrm{Corr}_{L_jG}(x))$, and the quality of the estimation must be maximum (1 if the quantification interval is [0, 1]). Two types of perturbations appear in the image:

- The image has at least three zones (at least two possible crop edges). The associated correlation function has the same number of maxima than the number of possible crop edges. We define a '*global adequacy coefficient*' $F = 1/q$ where q is the number of maxima of the correlation function for which the value is higher than $\epsilon.\mu_a$ ($\varepsilon \in [0, 1]$) is a sensibility coefficient).
- Gaussian noise appears in the image. The more significant the noise is, the more the value of the maximum of the correlation function is weak. We define a '*local adequacy coefficient*' $A = \mu_a/(2\beta) \in [0, 1]$).

Both the local adequacy coefficient and the global adequacy coefficient are important in order to quantify the quality of the estimation of the crop edge position.

2.3.2.2. The theory of evidence. Two principal theories can be distinguished in data fusion. The probability models represent the information into densities of probability (Haton, 1991). These models are however limited when some conflicting opinions must be merged or when the a priori information is unknown in the case of Bayes theory. Models based on the theory of evidence (Shafer, 1976; Bloch, 1996) are adapted for the estimation of the imprecision and the uncertainty.

We define Θ as the set of the possible positions of the crop edge: $\Theta = \{I_1,\ldots, I_m\}$ where $I_i(i\in\{1, \ldots, m\})$ is the hypothesis: 'the crop edge is a vertical line which passes by the image sites number i'. In the probability theory, we can only assign probability measures to elementary subsets (H_i). In the theory of evidence, belief can be assign to all the subsets of Θ (2^Θ subsets). So, uncertainty can be set if we assign belief to Θ. We can define $m{:}2^\Theta \rightarrow [0, 1]$ called mass function whenever:

$$m(\emptyset) = 0 \qquad \sum_{A \subset \Theta} m(A) = 1 \tag{4}$$

The quantity $m(A)$ is called A's basic probability number (basic belief or mass given to A), and it is understood to be the measure of the belief that is committed exactly to A. It is possible to combine mass functions by the orthogonal sum operator: consider two independent sources of information represented by their mass functions m_1 and m_2. Then m_1 and m_2 can be combined by:

$$m_{12}(z) = m_1(z) \oplus m_2(z) = K^* \sum_{(X,Y)/X\cap Y = z} m_1(X)^* m_2(Y) \tag{5}$$

where z is a subset of Θ, X and Y are different parts of the frame of discernment and with:

$$\frac{1}{K} = 1 - \sum_{(X,Y)/X\cap Y = \emptyset} m_1(X)^* m_2(Y) \tag{6}$$

The degree of conflict between the two sources can be evaluated with K. Before building the mass functions, let us compute probability distributions from the correlation functions:

$$\begin{aligned} C_j(x) &= \mathrm{rot}_{r\beta}\begin{Bmatrix} \mathrm{Corr}_{L_iG}(x) & \text{if} \quad \mathrm{Corr}_{L_jG}(x) > 0 \\ 0 & \text{Otherwise} \end{Bmatrix} \\ p_j(x) &= \frac{1}{\sum_{k=1\ldots m} C_j(k)} C_j(x) \end{aligned} \tag{7}$$

where $\mathrm{rot}_{r\beta}$ is the operator of right rotation of β terms. The aim of this transformation is to remove the offset created by the position of the transition in the reference vector. p_j is a probability density function associated with the parameter P_j. Let us define four mass functions m_1, m_2, m_3, m_4 where:

$$m_j(\Theta) = 1 - F_j.A_j \qquad m_j(x) = (1 - m_j(\Theta)).p_j(x) \tag{8}$$

where $m_j(\Theta)$ is the residual uncertainty of the estimation, and (F_j, A_j) are the global and local adequency coefficient associated with the parameter P_j. It is now possible to compute the global mass using the Dempster rule of combination defined in Eq. (5):

$$m = m_1 \oplus m_2 \oplus {}_3 m_4 \tag{9}$$

The value of $m(\Theta)$ is a good estimation of the reliability of the detection of the crop edge. The maximum of the mass function m indicates the most probable position of the crop edge.

Fig. 7 is an example of a crop edge detection in a image of grass vegetation. The low level algorithm computes four tables of parameters which are the same as used in the unsupervised method. We then compute four correlation functions between each parameter and the image model. Subsequently, these four correlation functions are transformed into four mass functions (Fig. 6). We can notice that the value of the residual uncertainty, $m(\Theta)$, is more important for the second moment and the homogeneity which are in this example, the two less representative parameters. The composed mass function can be computed by the Dempster's rule of combination. Results show that the maximum of belief is given for the position of the limit on the site number 19 with a value of residual uncertainty about 0.13. The right part of the Fig. 7 shows the final crop edge estimation calculated by the global algorithm. If all the parameters are unrepresentative, consequently the value of the global residual uncertainty will be high. If we set a threshold on it, it is possible to validate (or not) the estimation of the crop edge.

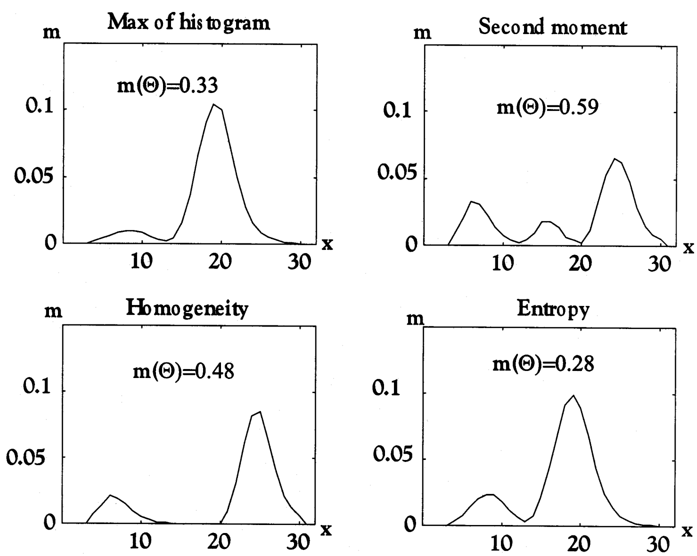

Fig. 6. Mass functions performed for the four parameters.

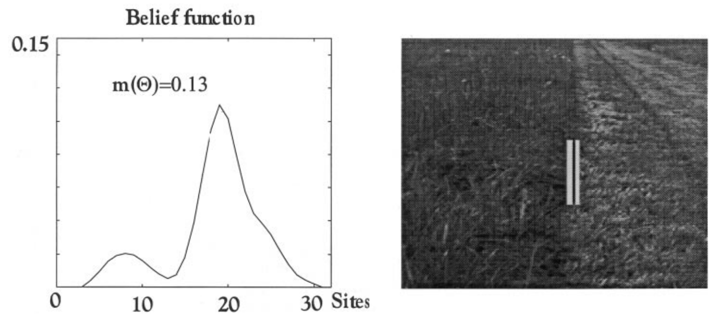

Fig. 7. Composed mass law and result of detection.

2.4. Discussion

If we have good results of image segmentation with the unsupervised method thanks to the use of texture parameters and Markov fields, it is sometimes difficult to find the good limit and we have no idea of the residual uncertainty of its position. The supervised algorithm has a principal characteristic: The use of the reliability criteria associated with each parameter is very important into the data fusion module. The estimation of a global criteria for the more probable position of the crop edge provides a control of the presence of the crop edge. In outdoor vision, where the quality of the acquisition depends on the relative position camera/sun, and where the number of types of pictures are very high, control of the reliability of the detection is essential. The guidance cannot be done correctly without this module. The vehicle is driven automatically via a closed servo-control loop. So, if the estimation is bad during four or five iterations, the crop edge can leave the image window and the guidance system will fail. If the algorithm detects the wrong estimation, it is possible to initially set the guidance-assistance system in a prediction mode, then in an alarm mode, so as to return control of the vehicle temporally to the driver.

3. Control laws

The guidance-assistance system sets two problems. The first one is the perception of the environment, the second one is the vehicle control. The consideration of these two difficulties shows the link between the second and the first problem. We add a feedback loop which makes it possible to correct errors and drifts of the system due to imprecise modeling and measures. Fig. 8 gives a system diagram of the application. From the visual information (θ and ρ, which are the coordinates of the crop edge in the image space), given by the image processing algorithm, we have designed well-adapted control laws for our applications. First, simple control laws based on a kinematic model of our machines have been developed. We present two of them which are tested on two vehicles (a mower and a combine harvester). The first one needs scene coordinates and uses the results of Kehtarnavaz in the BART project (Kehtarnavaz et al., 1991). The second control law is based on the visual servoing theory (Espiau et al., 1992) and uses only the coordinates given by the image frame. It has been developed for robot manipulators and we have adapted it for a non-holonomic mobile robot. In the two cases we do not need a dynamic model of our machines because of the low speed of agricultural machines ($\leq$ 10 km/h).

3.1. Control law with 3D trajectory

In this part, we present the definition of a trajectory which allows a vehicle to go from its initial position to a new position in front of it. We have tested this approach with a mower using application parameters (distance from image center and machine position, camera height…) which are adapted to a mower. However, the presented method is only dependent on the kinematic model of the machine and can be extended to other vehicles (tractor, combine harvester…). Our application uses a video sensor, so we have to eliminate all large movements of the vehicles to keep the crop edge in the image. To do that, the trajectory calculated needs to go from the initial position to the desired position with a large radius of curvature. The idea is to find two tangent circles, one of which includes the current position of the machine and the other the desired position (Fig. 9). Kehtarnavaz in (Kehtarnavaz

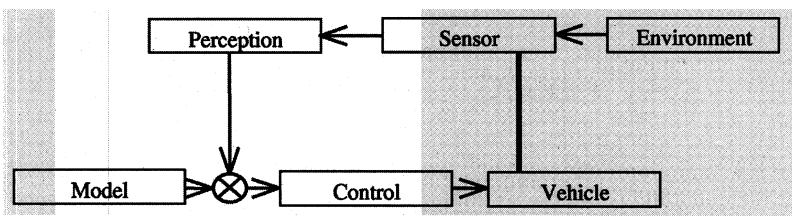

Fig. 8. General control diagram.

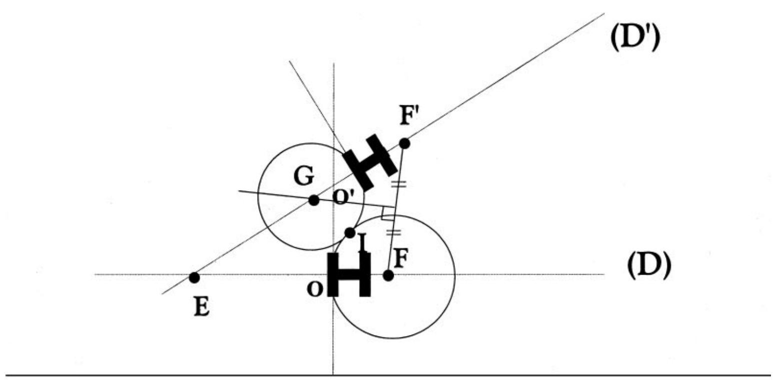

Fig. 9. Vehicle trajectory.

(a)

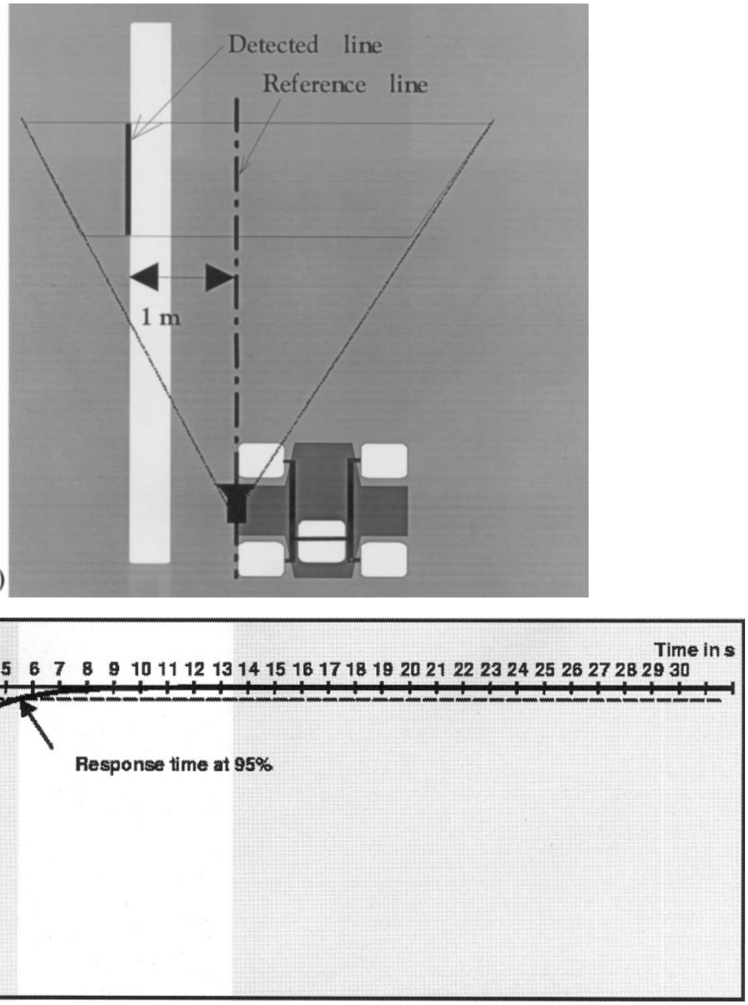

Fig. 10. Simulation conditions and response to a step of 1 m.

et al., 1991) uses circles with the same radius of curvature. So the radius of curvature is same in magnitude along all the trajectory. In our case we use another condition (Debain et al., 1994) which makes possible to maximize the radius of curvature. Then the trajectory followed by the machine is smoother and better for the image processing module. Using this control law, we have simulated the machine behavior at a speed of 3 km/h. Fig. 10 gives the response on a trajectory with a step of 1 m. This curve shows a good control of the machine which corrects the error of 1 m in less than 10 s. It also shows the method's stability because we do not notice any oscillation or overshoot. Some tests in real conditions have shown the same behavior as in simulation with a precision better than 10 cm. In this experiment, the camera is embedded on the mower (camera height = 100 cm, camera angle = 10°).

3.2. Control law in the image space

Our vehicles often work on bumpy ground which induces a lot of noise in the 3D point coordinates estimated from the image information. So we tried another control law which uses only image information. It has been developed for a farm robot. Many works concerning robot manipulators (Feddema et al., 1989; Espiau, 1993; Hashimoto, 1993; Corke, 1996; Hager et al., 1996; Chaumette, 1998) have shown the robustness of this control in relation to calibration errors and noise. However the visual servoing approach was not applicable to non-holonomic machines. So in our work, we have shown how we can use visual servoing to control the trajectory at constant speed of non-holonomic agricultural vehicle in the image space (Debain, 1996; Khadraoui et al., 1998; Martinet et al., 1998). From the interaction matrix and the task function approach developed by Espiau and Samson (Samson et al., 1991), we deduced a control law which gives the camera rotation as a function of the detected line coordinates in the image frame:

$$\Omega_y = \lambda \left[\beta \frac{\sin\alpha\cos\alpha}{1+h^2}(\theta-\theta*) + \frac{h^2+\cos^2\alpha}{1+h^2}(\rho-\rho*) \right] \tag{10}$$

with:

- α, angle between the ground plan and the camera axis;
- h, camera height;
- ρ and θ, coordinates of the detected line in the image space;
- λ and β are gains which depend on the vehicle model and the desired response curve.
- ρ^* and θ^* are the polar coordinates of the detected line when the machine is well-controlled (reference line in image space).

3.2.1. Application

We use this formalism to control the trajectory of a combine harvester. To do that, we search a kinematic model (Fig. 11) of the vehicle described in (Debain, 1996; Khadraoui et al., 1998). Then we find the equation which gives the control values:

$$\begin{cases} v = v_{\text{moy}} \\ \tan\delta = \dfrac{L.\Omega_y}{v_{\text{moy}}} \end{cases} \tag{11}$$

with:

- v_{moy}, vehicle mean speed;
- L, distance between the axles;
- v and δ, vehicle control variables.

So we have a relation between the control variables of the vehicle and the polar coordinates of the detected line given in the image frame. It should be noticed that we consider that the speed of the machine is constant and non-zero.

3.2.2. Simulation tests

First we make simulation tests in which the machine has to reach a line 1 m away (Fig. 12). Like for the mower experiments, the camera is embedded on the combine (camera height = 3 m, camera angle = 25°). We have several test conditions which makes possible to adjust our gains according to the desired curve of response (Fig. 13). For our simulations, we choose a speed of 4 km/h and the sampling period is about 100 ms. On the curve, we see the machine error between its current position and the line position. From $t = 7$ s we can see the response to the step which is about 20 s.

3.2.3. Tests in real conditions with the machine

After the simulation tests it was interesting to make real tests. To do that, we decided to follow a white line on the ground to optimize the precision of the visual

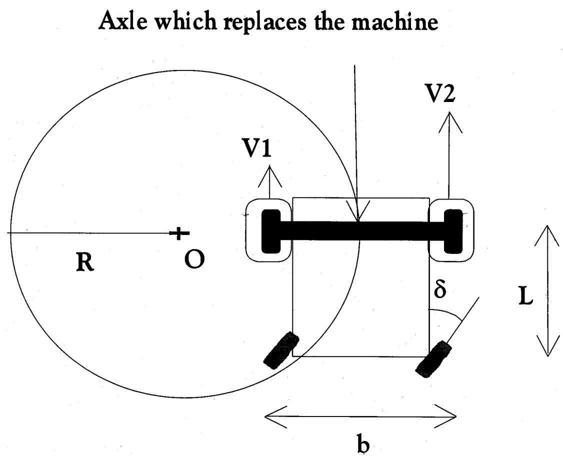

Fig. 11. Vehicle model.

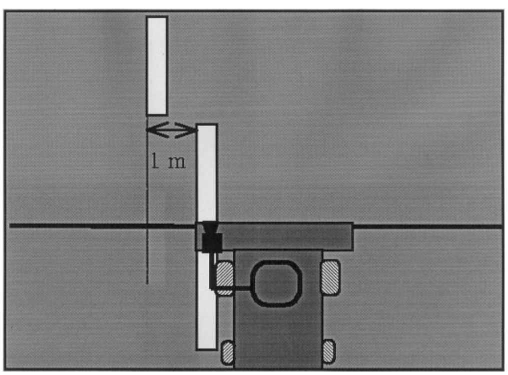

Fig. 12. Simulation and real test conditions.

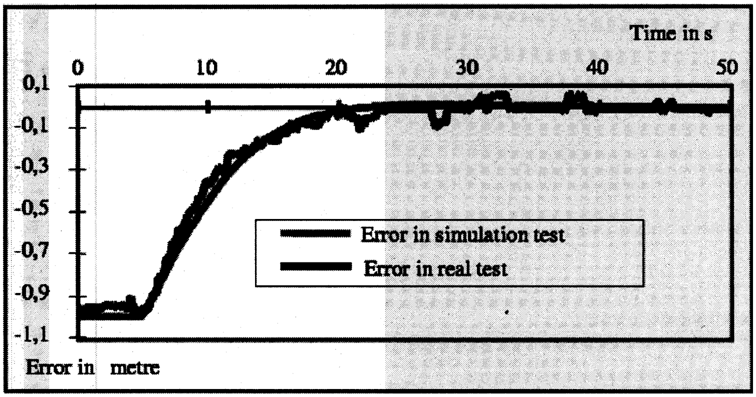

Fig. 13. A real test at 4 km/h.

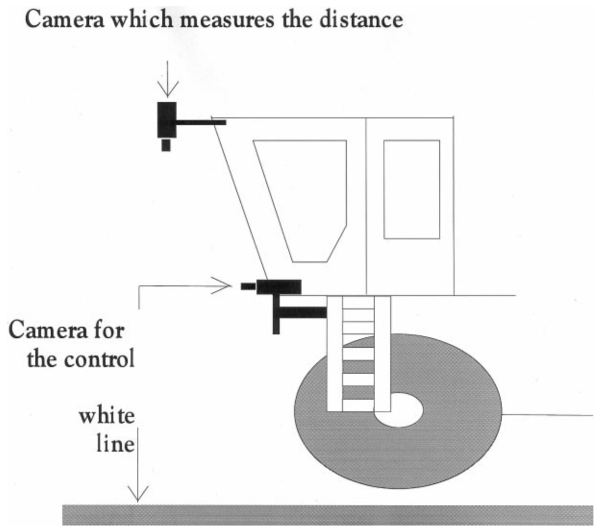

Fig. 14. Two cameras: one to guide, one to measure the result.

perception algorithm, because it is easier to detect a white line than a limit between mowed and unmowed vegetation. We have made tests in various conditions (with or without additional noise: 20%) at different speeds and with a sampling period which changes with time.

The quality of our control servoing can be calculated in real time by using a second camera which is continuously measuring the distance between the vehicle and the white line (Fig. 14).

The curve is done at a speed of 4 km/h and a sampling period of 100 ms which represents the image processing calculation time (Fig. 13). For the simulation needs, we introduce a delay corresponding to the image processing calculation time. We can thus compare the simulation and the real curve which are done in the same experimental conditions. We can notice that the real and simulation curves are superimposed. The response time is about 20 s and there is not any overshoot. There is a lot of noise on the real curve because the camera which measures the distance between the vehicle and the white line vibrates when the machine runs. The same image processing algorithm is used to control the machine and to measure the error. This algorithm has a precision better than 10 cm. So the most part of the noise is produced by the camera and the image processing algorithm which measure the distance between the vehicle and the white line.

3.3. *Visual servoing in difficult conditions*

Agricultural vehicles often work on sloping ground. So we tested our visual servoing control law on this condition in simulation and real tests. In Fig. 15 we can observe the machine behavior on sloping ground with a classical guidance-assistance system using visual servoing. The machine has to follow a white line drawn

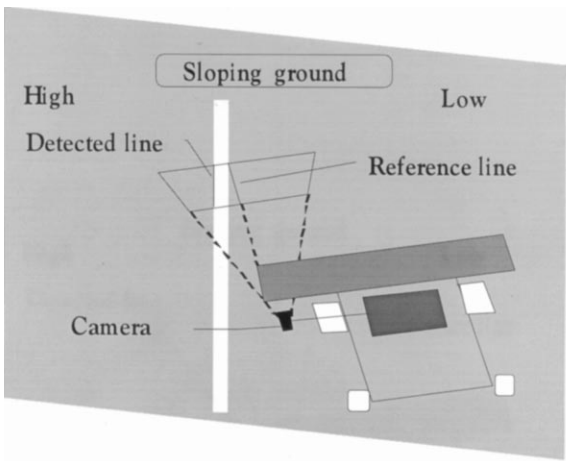

Fig. 15. Automatic driving.

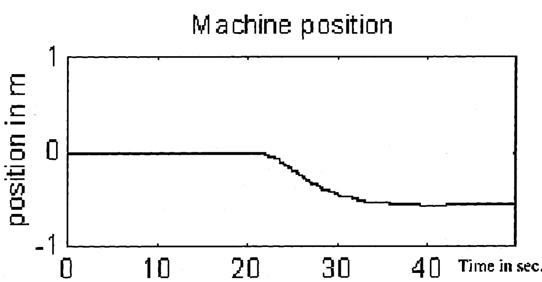

Fig. 16. Distance between the machine and the line.

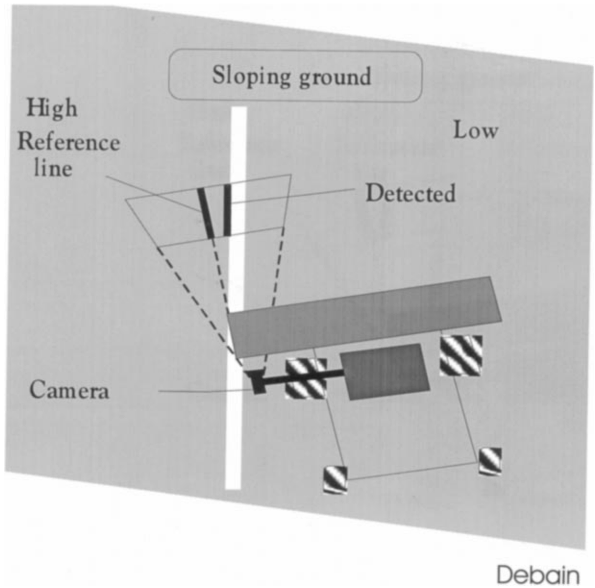

Fig. 17. Manual driving.

on the ground. Fig. 16 gives the distance between the machine position and the white line. When the slope appears (at $t = 20$ s) there is a constant error in the position of the machine. We can also see that the machine is not parallel to the white line (Fig. 15). There is an angle between the direction of the white line and the machine orientation. And we can say that this angle depends on the slope and the sliding conditions. With the same experimental conditions, and if the machine is driven by a person, we observe an angle between the white line and the machine orientation (Fig. 17). It is the same angle as we observe for the case of the Fig. 15. So we can say that there is a relation between this angle and the slope of the ground. In fact, the driver corrects the slope effects by shifting the machine. But with the guidance-assistance system there is a constant error at the end of the cutter bar divider (a tool of the combine) in the case of a combine harvester, due to the slope and the sliding conditions. Our idea is to read the slope effects through the angle between the machine orientation and the white line. We have to find a link between this angle and the constant error observed with the guidance system. To do that, it is interesting to note that the position of the detected line is not the same in the two cases. When the machine is correctly guided along the white line (Fig. 17), the reference line is not superimposed on the detected line. So the reference line which is the line detected when the machine is correctly guided is not the same for sloping ground (Fig. 18, right) and a flat ground (Fig. 18, left). We have shown that the reference lines are not the same if the machine runs on flat ground or sloping ground. Then we have noticed that the slope effect on the vehicle behavior can be described by an orientation of the machine. To find the set of all the reference lines

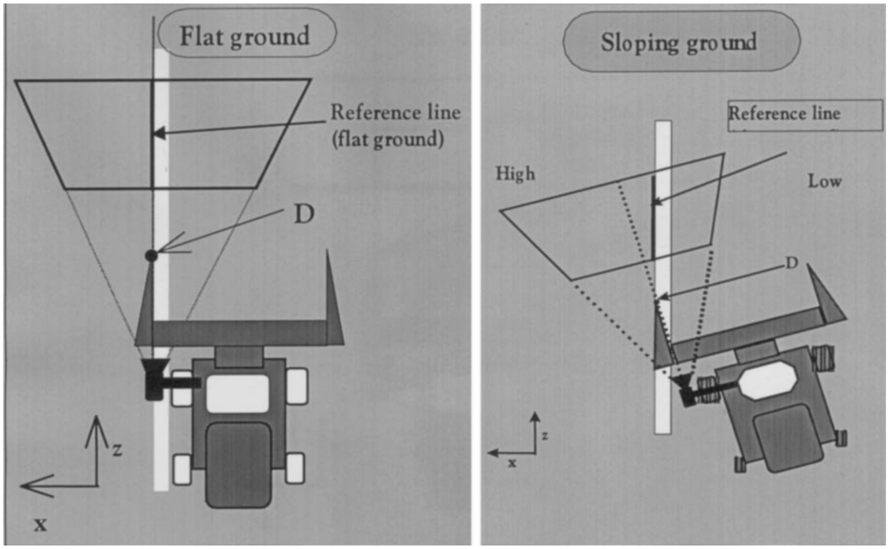

Fig. 18. Two reference lines for two different situations.

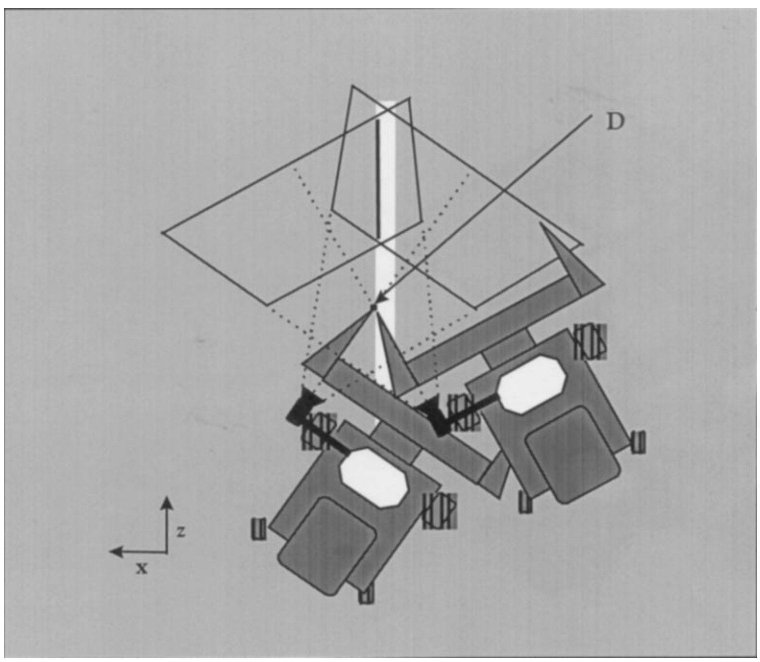

Fig. 19. Several positions.

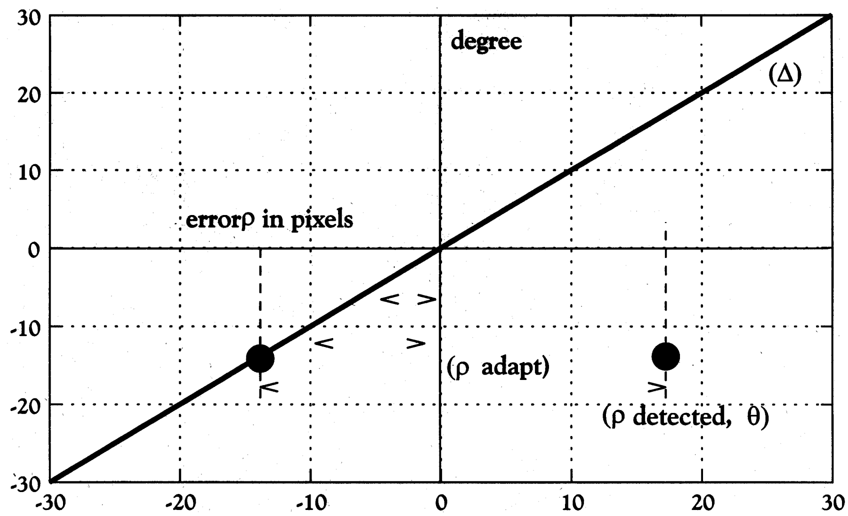

Fig. 20. Set of the 2D parameters for each slope value.

which give the coordinates of the detected line in the image when the machine is correctly controlled, we have recorded the image parameters (ρ, θ) for several slope values (Fig. 19). The graph of these parameters is given in Fig. 20. It is a straight line and the point (0, 0) represents the coordinates of the reference line for a flat ground.

Then the difficulty is to find the coordinates of the reference line that represents the current situation (the slope of the ground and the sliding conditions). To do that, we use the orientation of the vehicle which is the consequence of the slope effects. Then, with this orientation we obtain the coordinates of the reference line (Fig. 20). So we obtain new values for the input of the control law (ρ_{adapt}, θ).

Our control law is a vision based control law. Many authors use a proportional vision based control law (Chaumette, 1990; Corke, 1993; Khadraoui et al., 1996). Due to the slope effect, an integrator module becomes necessary in the control law. In addition, with this module, it is possible to have a constant steering angle even if the error is equal to zero. The details of the proportional integral law calculation is given in (Debain, 1996). We just give the result, that means the equation between the steering angle of the vehicle and the visual information:

$$\delta = -\frac{\lambda.L}{v_{\text{moy}}}\left[\beta\,\frac{\sin\alpha\cos\alpha}{1+h^2}\,\theta + \frac{h^2+\cos^2\alpha}{1+h^2}\left(\rho_{\text{adapt}} + k_i.\int_0^t \rho_{\text{adapt}}\,du\right)\right] \tag{12}$$

where λ, β and k_i are three gains which control the behavior of the vehicle and (ρ, θ) are the polar coordinates of the line detected in the image.

Fig. 21 gives a view of the visual guidance system which controls an agricultural vehicle on sloping ground. With a such corrector we have good results in simulation and real conditions. For example, in the Fig. 22 we can see that when we use the corrector (at $t = 50$ s), we correct the slope effect in 5 s. Fig. 23 shows the control

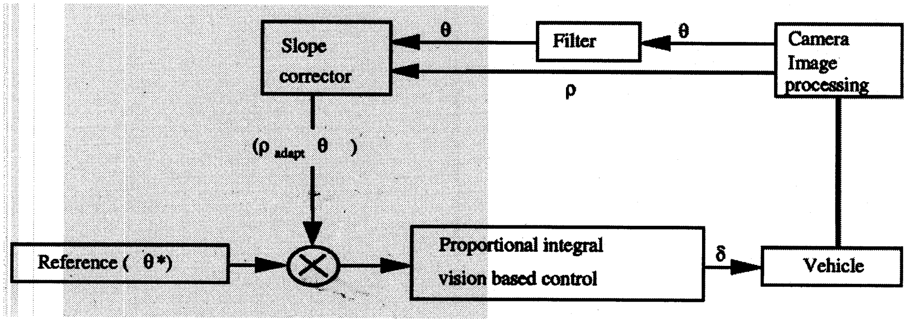

Fig. 21. The visual guidance system with the slope corrector.

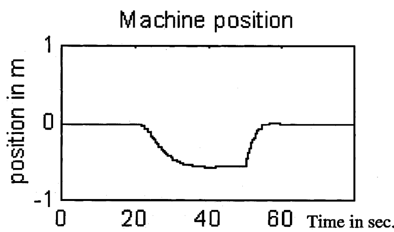

Fig. 22. Simulation result with the slope corrector.

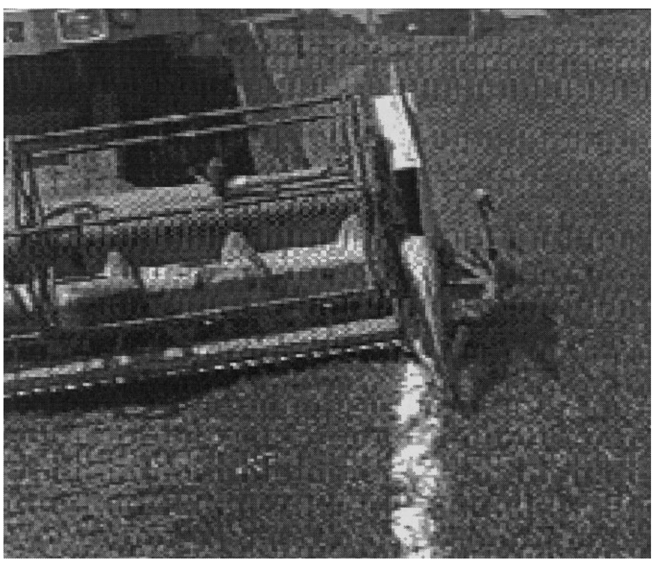

Fig. 23. Result in real condition.

of a combine harvester on sloping ground. We can see the angle between the machine and the white line it has to follow. We observe that the vehicle is correctly controlled with a precision better than 10 cm. In these two examples the slope is about 20%. So we found a solution to guide a mobile robot on sloping ground by using only the sensor of the visual guidance system. To do that we make the hypothesis that the machine has to follow a line locally approximated by a straight line. For many agricultural applications, this hypothesis seems to be sufficient. To correct the sloping ground effects we use only the machine orientation which gives us the new steering angle. We made tests in simulation and real conditions. The results show a good behavior of the machine which is robust from different slopes and sliding conditions.

4. Summary and conclusion

In this article, we present different works we have done on a guidance-assistance system for two agricultural vehicles. We show different difficulties found in our projects. Firstly the environment perception described by means of image processing algorithms which use supervised or unsupervised methods. In this part we notice the need to qualify the reliability of the perception information in order to guide correctly the vehicles. To do that, we give a solution using the theory of evidence which formalizes the uncertainty and computes a reliability criterion associated with the estimation of the crop edge. Secondly, two control laws determine the orders of the machine steering angle to guide them along the crop edge. The first one consists to generate a reference trajectory and the second one, which is calculated in the image space, can be used in very difficult situation like sloping ground. The result satisfies most situations and the precision of the system is better than 10 cm. Nevertheless, there are still very difficult situations in which it is impossible to correctly guide agricultural vehicles (sun direction at the end of the afternoon, shadow of the machine in the image, lack of vegetation). Future works will increase the environment perception using others sensors like laser telemeter and fuzzy based theory to combine laser and video information. We will also work on guidance-assistance system by CPDGPS and new control algorithms in 3D space.

References

Amat, J., Battle, J., Fuertes, J.M., Martinez, A., 1993. Vision controlled robot for agricultural application. Proceedings of the 24th ISIR, pp. 537–542.

Billingsley, J., Schoenfisch, M., 1997. The successful development of a vision guidance system for agriculture. Comput. Electron. Agric. 16, 147–163.

Bloch, I., 1996. Incertitude, imprécision et additivité en fusion de données: point de vue historique. Traitement du signal 13, 268–288.

Chateau, T., Berducat, M., Bonton, P., 1997. An original correlation and data fusion based approach to detect a reap limit into grey level image. In: Proc. IEEE Int. Conf. Intelligent Robots and Systems, vol. 3. IROS'97. Grenoble, France, pp. 1258–1263.

Chaumette, F., 1990. La relation vision-commande: théorie et application à des tâches robotiques. PhD thesis. IRISA/INRIA-Rennes. Rennes, France.

Chaumette, F., 1998. Potential problems of stability and convergence in image based and position-based visual servoing. The confluence of Vision and Control, LNCIS series, Springer Verlag.

Cohen, F.S., Cooper, D., 1987. Simple parallel hierarchical and relaxation algorithms for segmenting non-causal markovian random fields. IEEE Trans. Pattern Analysis and Machine Intelligence 19 (2), 195–219.

Corke, P., 1993. Visual control of robot manipulators-A review, vol. 7 of Robotics and Automated Systems, ISBN 981-02-1864-6, World Scientific Publishing Co., pp. 1–31.

Corke, P.I., 1996. Visual Control of Robots: High Performance Visual Servoing. Research Studies Press, ISBN 0-86380-207-9, John Wiley.

Debain, C., 1996. Lois de commande pour le contrôle et la mobilité de machines agricoles. PhD thesis. Université Blaise-Pascal, Clermont-Ferrand, France.

Debain, C., Derras, M., Berducat, M., Bonton, P., Gallice, J., 1994. Development of a visual guidance system for an upkeep robot of natural environments. In: Proc. Int. Symp. Signal Processing, Robotics and Neural Networks, IMACS, Lille, France, pp. 121–124.

Derras, M., 1993. Segmentation non-supervisée d'images texturées par champs de Markov: application a l'automatisation de l'entretien des espaces naturels. PhD thesis, Université Blaise-Pascal, Clermont-Ferrand, France.

Derras, M., Berducat, M., Bonton, P., 1991. Image processing and algorithm merging: real time control of an unkeep machine for natural space. In: Proc. IARP Workshop on Robotics in Agriculture and Food Industries, pp. 10–18.

Derras, M., Debain, C., Berducat, M., Bonton, P., Gallice, J., 1994. Unsupervised regions segmentation: real time control of an upkeep machine of natural space. In: Proc. Eur. Conf. Computer Vision, pp. 207–212.

Espiau, B., 1993. Effect on camera calibration errors on visual servoing in robotics. In: Proc. Third International Symposium on Experimental Robotics, pp. 187–193.

Espiau, B., Chaumette, F., Rives, P. 1992. A new approach to visual servoing in robotics. IEEE Trans. on Robotics and Automation, vol. 8 (3).

Feddema, J.T., Lee, C.S.G., Mitchell, O.R., 1989. Automatic selection of image features for visual servoing of a robot manipulator. In: Proc. IEEE Int. Conf. Robotics and Automation, Scottsdale, Arizona, pp. 832–837.

Hager, G.D., Hutchinson, S., Corke, P., 1996. Visual servo control. IEEE Int. Conf. Robotics and Automation. Minneapolis Hilton and Towers, Minneapolis, Minnesota (Tutorial TT3).

Haralick, R.M., 1979. Statistical and structural approaches to texture. Proc. IEEE, pp. 786–804.

Hashimoto, K., 1993. Visual Servoing: Real-time Control of Robot Manipulators Based on Visual Sensory Feedback, vol. 7 of Robotics and Automated Systems, ISBN 981-02-1364-6, World Scientific Publishing Co.

Haton, J., 1991. Le raisonnement en intelligence artificielle, ISBN 2–7296-0335-2612293-1, InterEditions.

Jarvis, R.A., 1990. Omniscient camera based outdoor mobile robot. In: Proc. Workshop on Robotics in Agriculture and the Food Industry. 1st IARP, Avignon-France, pp. 247–258.

Kehtarnavaz, N., Grisworld, N., Lee, J., 1991. Visual control for an autonomous vehicle (BART) — the vehicle following problem. IEEE Trans. Vehic. Technol. 40 (3), 654–662.

Khadraoui, D., Debain, C., Rouveure, R., Martinet, P., Bonton, P., Gallice, J., 1998. Vision based control in driving assistance of agricultural vehicles. Int. J. Robot. Res. 17 (10), 1040–1054.

Khadraoui, D., Motyl, G., Martinet, P., Gallice, J., Chaumette, F., 1996. Visual servoing in robotics scheme using a camera/laser–stripe sensor. IEEE Trans. Robot. Automat. 12 (5), 743–750.

Klassen, N.D., Wilson, R., Wilson, J., 1994. Guidance systems for agricultural vehicles. In: Proc. 12th World Cong. on Agricultural Engineering, International Commission of Agricultural Engineering, Milano, Italia, pp. 1136–1142.

Liu, W., 1994. Détection par mesure de non stationarité locale: application a la segmentation de signaux multi-dimensionnels. PhD thesis, Insa, Lyon, France.

Marchant, J., Hague, T., Tillet, N., Sanchez, J., 1997. Research on autonomous vehicle for precise plant treatments. In: Proc. Int. Workshop on Robotics and Automated Machinery for bio-production, Valencia, Spain, pp. 237–242.

Martinet, P., Bonton, P., Gallice, J., Berducat, M., Debain, C., Rouveure, R., 1998. Automatic guided vehicles in agricultural and green space fields. In: Proc. 4th French-Israeli Symp. on Robotics. FIR'98. Besançon, France, pp. 87–92.

Max, J., 1985. Méthodes et techniques de traitement du signal et application aux mesures physiques, ISBN 2-225-80470-2, Masson, Milan.

Nobutaka, I., 1990. Agricultural robots applications in japan. In: Proc. IARP Workshop on Robotics in Agriculture and Food Industry, Avignon, France, pp. 35–44.

Ollis, M., Stentz, A., 1996. First results in vision based crop line tracking. In: Proc. IEEE Int. Conf. on Robotics and Automation, vol. 1. Minneapolis, Minnesota, USA, pp. 951–956.

Ollis, M., Stentz, A., 1997. Vision based perception for an automated harvester. In: Proc. IEEE Int. Conf. on Intelligent Robots and Systems, vol. 2. IROS'97. Grenoble, France, pp. 1838–1844.

Samson, C., Le Borgne, M., Espiau, B., 1991. Robot Control. The task function approach. ISBN 0-19-8538057. Clarendon Press, Oxford.

Sanchez, A., Marchant, J., 1997. Fast and robust method for tracking crop rows using a two point through transform. In: Proc. Int. Workshop on Intelligent Robotics and Automated Machinery for Bio-production, Valencia, Spain, pp. 28–33.

Shafer, G., 1976. A mathematical theory of evidence, vol. 2702. Princeton University Press, New Jersey.